Journal of Catalysis **186,** 188–200 (1999)
Article ID jcat.1999.2554, available online at http://www.idealibrary.com on IDEAL®

Dehydroisomerization of *n*-Butane over Pt–ZSM5 (I): Effect of the Metal Loading and Acid Site Concentration

G. D. Pirngruber,* K. Seshan,* and J. A. Lercher*,†

*Faculty of Chemical Technology, University of Twente, P.O. Box 217, 7500 AE Enschede, The Netherlands; and †Institute for Chemical Technology, Technical University of Munich, Lichtenbergstr. 4, D-85748 Garching, Germany

Received February 17, 1999; revised April 28, 1999; accepted April 28, 1999

The dehydroisomerization of *n*-butane to isobutene over Pt–ZSM5 catalysts with a high Si/Al ratio was studied. The catalytic activity increases with increasing metal loading. Butenes formed via dehydrogenation over the metallic particles are converted to isobutene over the Brønsted acid sites. The molar fraction of isobutene (in all butenes), which can be taken as a measure for the isomerization activity, increases parallel to the acid site concentration, but is independent of the metal loading. The highest yields of isobutene achieved at 830 K, at 1.8 bar, and with a feed of 10% *n*-butane and 20% hydrogen were approximately 12.5%. The thermodynamic limit under these conditions is about 22%. The inability to reach the thermodynamic limit is caused by consumption of the primarily formed *n*-butene by secondary side reactions. The major side reactions are oligomerization and cracking of butenes over Brønsted acid sites leading to propene and pentene. Propene that is formed via this route is hydrogenated to propane over Pt. Consequently, propane is the dominant by-product at high conversions. The metal loading has only a minor influence on the selectivity of the catalyst.

INTRODUCTION

Isobutene is a very important intermediate in the petrochemical industry, mainly used for the production of polymers (butyl rubber, polybutene, and isoprene) and of MTBE. In 1984, 1.2×10^6 tons (t) of isobutene were used for the production of butyl rubber, polybutene, and isoprene, 1.0×10^6 t for the production of MTBE (1). Currently, the world demand for MTBE is estimated to be 1.2×10^7 t/year, corresponding to an isobutene consumption of 7.8×10^6 t/year (2). Legislative changes, however, may shift this demand (3).

In the refinery, isobutene is produced in the FCC process. As it is a by-product, the capacity cannot be easily expanded. Thus, dehydrogenation of butanes is the prevailing production route. This route comprises two separate steps. *n*-Butane is isomerized, then the isomers are separated by distillation, and isobutane is passed on to a dehydrogenation unit where it is converted to isobutene. Attempts have been made to combine these two steps and to design a catalyst (process) that is able to directly convert *n*-butane to isobutene. Two different concepts have been followed, using either a two-bed reactor with a dehydrogenation catalyst in combination with an isomerization catalyst or a truly bifunctional catalyst, usually a metal/zeolite combination. The most successful example for a two-bed system has been published by Bellussi *et al.* (4). They used Pt impregnated on a silylated alumina carrier (with In and Sn as promoters) as a dehydrogenation catalyst and added a bed of Boralite B to increase the isobutene yield. Nagata *et al.* (5) found good results for a combination of Cr_2O_3/Al_2O_3 with MFI-type metallosilicates with a very high Si/Me ratio of 1000. Recently, the combination of Zn/K–ZSM5 with H–ZSM22 was reported (6).

With respect to the bifunctional catalysts, mainly zeolite-based materials have been explored, e.g., Pt–MOR (7), Ga–LTL (8), and Pt–zincosilicate (9). The highest isobutene yield (10%) was obtained with a Pt/Re–{B}–ZSM11 catalyst (10).

It is generally assumed that with a bifunctional catalyst the dehydrogenation over the metal is the first reaction step, followed by isomerization over the Brønsted acid sites. The reaction is usually carried out at elevated temperatures, as a consequence of the more favorable thermodynamics for butane dehydrogenation. Addition of hydrogen is not desirable from a thermodynamic point of view, but it is necessary to prevent extensive coking of the catalyst. Cracking, hydrogenolysis, and coking are possible side reactions that affect selectivity and the lifetime of the catalyst.

The aim of the present contribution is to describe the influence of the catalyst variables (such as the concentration of acidic and metallic sites) upon the complex network of reactions during *n*-butane dehydroisomerization. This leads to clear guidelines for designing the bifunctional dehydroisomerization catalyst. As a base case catalyst, we chose Pt supported on/in H–ZSM5 as preliminary screening experiments and literature reports suggest that it is a suitable material (9, 11, 12).

0021-9517/99 $30.00

EXPERIMENTAL

Catalyst Preparation and Characterization

The parent ZSM5 materials with a SiO_2/Al_2O_3 ratio of 480, 125, and 80 were supplied by ZEOLYST (sample codes CBV10002, CBV15014, and CBV8014, respectively). Pt was incorporated by liquid-state ion exchange. A highly diluted solution of $Pt(NH_3)_4(OH)_2$ (0.1–0.2 mg of Pt/ml) and ammonia (concentration approximately 2%) was added dropwise to a suspension of ZSM5 in water (10 ml of H_2O/g of zeolite) over a period of several hours. The addition of ammonia to the solution slows down the ion-exchange reaction and is supposed to give a better dispersion of the Pt complex over the zeolite pores (13, 14). The suspension was stirred for 20 h at room temperature. The final pH was typically between 8 and 9. After filtration, the filter cake was washed twice with doubly distilled water. The sample was dried, slowly heated in flowing air to 723 K (0.5 K/min), and kept at this temperature for 2 h to decompose the Pt complex. After cooling down to ambient temperature, the calcination tube was flushed with nitrogen. Finally, the sample was reduced in flowing H_2 for 2 h at 773 K (5 K/min) (15).

Samples with Pt loadings between 0.1 and 1.0% were prepared. The samples were characterized by chemical analysis (XRF), IR spectroscopy, and hydrogen chemisorption. Hydrogen chemisorption was carried out in a volumetric system. About 1 g of the sample was reduced for 1 h at 823 K in H_2. After reduction, the sample was degassed at 823 K for 1 h in a vacuum (10^{-5} mbar). The rather high temperature of 823 K was chosen for reduction and degassing because the dehydroisomerization reaction was also performed at high temperatures (830 K, *vide infra*). After degassing, the sample was cooled to room temperature and the hydrogen adsorption isotherm was measured by dosing decreasing amounts of H_2 (in the range of 500–50 mbar) to the sample. The hydrogen chemisorption capacity was calculated by extrapolation of the hydrogen uptake to zero pressure (16). In spite of the high temperatures used for reduction, rather high metal dispersions were measured for all the samples (see Table 1).

To characterize the Brønsted acidity of the catalysts, IR spectroscopy was employed. The samples were activated *in situ* in a flow of He or H_2 (for the metal-exchanged samples) at 823 K for 1 h and then cooled down to 573 K, where a spectrum of the catalyst was taken. Different samples were normalized by the intensity of two bands at 1975 and 1865 cm^{-1}, attributed to the overtones of lattice vibrations. The number of Brønsted acid sites was estimated by the relative intensity of the ν(OH) band at 3610 cm^{-1}, using CBV8014 as a reference. For this sample, the concentration of acid sites had been determined by gravimetry (17) to be 0.400 mmol/g. Since this number was in excellent agreement with the Al content determined by XRF (0.405 mmol/g), it was concluded that very little extraframework aluminum was present and that all the acid sites were indeed Brønsted acid sites, making the catalyst a suited reference material.

TABLE 1

Physicochemical Characterization of the Pt–ZSM5 Samples

Sample	SiO_2/Al_2O_3	Al (mmol/g)	H^+ (mmol/g)[a]	% Pt	H/Pt
0.1% Pt–ZSM5(480)	480	0.070	0.021	0.09	>2.0
0.3% Pt–ZSM5(480)	480	0.068	0.023	0.27	1.2
0.5% Pt–ZSM5(480)	480	0.069	0.023	0.46	1.15
0.1% Pt–ZSM5(125)	125	0.257	n.d.	0.09	n.d.
0.3% Pt–ZSM5(125)	125	0.257	n.d.	0.29	n.d.
0.5% Pt–ZSM5(125)	125	0.259	0.194	0.48	0.66
1% Pt–ZSM5(125)	125	0.257	n.d.	0.89	0.72
0.1% Pt–ZSM5(80)	80	0.404	n.d.	0.10	n.d.
0.5% Pt–ZSM5(80)	80	0.404	0.348	0.53	1.2
1% Pt–ZSM5(80)	800	0.409	0.377	1.04	0.74

Note. n.d., not determined.

[a] Determined by the intensity of the ν(OH) band at 3610 cm^{-1}, using ZSM5(80) as a reference.

The results of XRF, IR spectroscopy, and hydrogen chemisorption are summarized in Table 1. In the following text, the samples will be denoted "*x*% Pt–ZSM5(*y*)" where *x* is the Pt loading in wt% and *y* is the SiO_2/Al_2O_3 ratio.

With 0.3% Pt–ZSM5(480) sodium ion exchange was performed to neutralize available Brønsted acid sites. For this purpose, the sample was stirred at room temperature in a 0.04 M solution of $NaNO_3$ for 24 h (the volume was chosen such as to have a 20-fold excess of sodium ions compared to the number of acid sites). The suspension was filtered and washed with water. The degree of ion exchange was checked by IR spectroscopy.

Catalytic Testing

For the catalytic tests, the samples were pressed, crushed, and sieved to obtain particle sizes in the range of 300–600 μm. Then, 10–100 mg of the catalyst were mixed with about 100 mg of quartz and filled into a quartz tube with an inner diameter of 4 mm. The catalyst bed had a typical length of 5–15 mm and was supported on both sides by quartz wool.

The samples were reduced *in situ* at 830 K for 1 h in a mixture of H_2/Ar (18/82). The oven temperature was controlled via a thermocouple placed on the outside of the reactor. Two additional thermocouples were placed on the top and on the bottom of the catalyst bed to measure the actual temperature. The difference between these two thermocouples was not higher than 4 K. The reaction was started by switching from H_2/Ar to the feedstream, which was under standard conditions a mixture of 10% *n*-butane, 20% H_2, and the rest Ar. The total flow was between 15 and 180 ml/min. The outlet pressure of the reactor was regulated by a back

pressure regulator, usually to 1.8 bar. The pressure drop over the reactor was not higher than 0.1 bar, in most cases, much less than that.

The reaction was usually followed for at least 2.5 h. In the first 10 min on stream, the reactor effluent was stored in sample loops for later analysis. After 10 min, the reaction products were analyzed by online gas chromatography. The samples were simultaneously injected into an Al_2O_3 PLOT column connected to an FID detector for measuring the hydrocarbons, and a combination of a Hayesep C with a MS5 Å column, connected to a TCD detector, for measuring H_2 (and *n*-butane). Before the reaction was started, the feed was analyzed via a bypass line. The TCD was used for the determination of the absolute concentrations of hydrogen (bypass and reaction) and *n*-butane (bypass). It was calibrated by means of reference gas mixtures. The FID was used to determine the relative concentrations of all hydrocarbons during the reaction.

Conversion and yields were calculated on a carbon basis, using the FID areas A_i and the corresponding response factors rf_i.

$$\text{Conversion} = \left[1 - A_{n\text{-}C_4} \times rf_{n\text{-}C_4} \Big/ \sum (A_i \times rf_i)\right] \times 100\% \quad [1]$$

$$\text{Yield}_i = A_i \times rf_i \Big/ \sum (A_i \times rf_i) \times 100\%$$

RESULTS

Characterization of Brønsted Acidity

For ZSM5(125), the relative intensity of the Brønsted (OH) band at 3610 cm^{-1} was in good agreement with the relative Al content (using ZSM5(80) = CBV8014 as a reference; see Table 2), indicating that also here only minor concentrations of extraframework aluminum were present. The large discrepancy for ZSM5(480) may be explained by the large error of both the XRF and the IR measurement at these low Al contents.

After Pt ion exchange and reduction, the number of Brønsted sites was reduced by 10–20% (see Table 3). The sodium-exchanged 0.3% Pt–ZSM5(480) had a relative (OH) intensity of 0.4, i.e., about 50% of the Brønsted acid sites had been exchanged.

TABLE 2

Relative Al Content and the Relative Intensity of the ν(OH) Band at 3610 cm^{-1} for the Parent ZSM5 Samples

SiO_2/Al_2O_3	480	125	80
Al content	0.173	0.635	1.000
ν(OH)	0.07	0.57	1.00

TABLE 3

Relative Intensity of the ν(OH) Band at 3610 cm^{-1} of the Parent and the Pt-Impregnated ZSM5 Samples

SiO_2/Al_2O_3	480	125	80
Parent	1.00	1.00	1.00
0.1% Pt	0.73	n.d.	n.d.
0.3% Pt	0.81	n.d.	—
0.5% Pt	0.78	0.84	0.86
1% Pt	—	n.d.	0.93

Time-on-Stream Behavior in Dehydroisomerization of n-Butane

Figure 1 shows the conversion and the yield of the main products obtained with 0.1% Pt–ZSM5(480) at two different weight hourly space velocities (WHSV). At a WHSV of 86 h^{-1}, butane was almost exclusively (96% selectivity) converted to butene and butadiene (about 0.5% yield); 18% of the butene fraction was isobutene. The catalyst deactivated with time on stream (the activity decreased by about 30% with 2.5 h).

At a WHSV = 9.5 h^{-1}, the catalyst was more stable (Fig. 1b). While the conversion slightly decreased with time on stream, the yield of butenes was stable at 32%; 36% of the butenes were isobutene. The selectivity to by-products, however, drastically increased compared to WHSV = 86 R^{-1}. The main by-products were propane, propene, ethane, methane, pentene, and isobutane (in the order of their rates of formation; see Fig. 1c). At a WHSV = 86 h^{-1}, the order of by-products[1] was propene, methane, ethane, and pentene, i.e., the by-product spectrum shifted in favor of propane and ethane with decreasing WHSV. For both WHSVs, the selectivity to by-products, especially to ethane, propane, and isobutane, decreased, as the catalyst deactivated.

A similar time-on-stream behavior was found for all catalysts measured. All of them showed slow deactivation with time on stream (not taking into account the induction period in the first few minutes). At high conversions, mainly the by-product formation decreased with time on stream while constant yields of total butenes and of isobutene were obtained.

To account for the slow deactivation described above, all experiments were compared at two points, (i) at zero time on stream and (ii) after 100 min time on stream, when all catalysts were in a quasi steady state. Since the same trends were observed for both methods of analysis, only the steady state values will be discussed in the following.

Activity for Dehydrogenation and Isomerization

Figures 2 and 3 show the influence of metal loading on *n*-butane conversion, butene and isobutene yields, and on

[1] Since none of these by-products has a yield higher than 0.4%, they are not shown in Fig. 1.

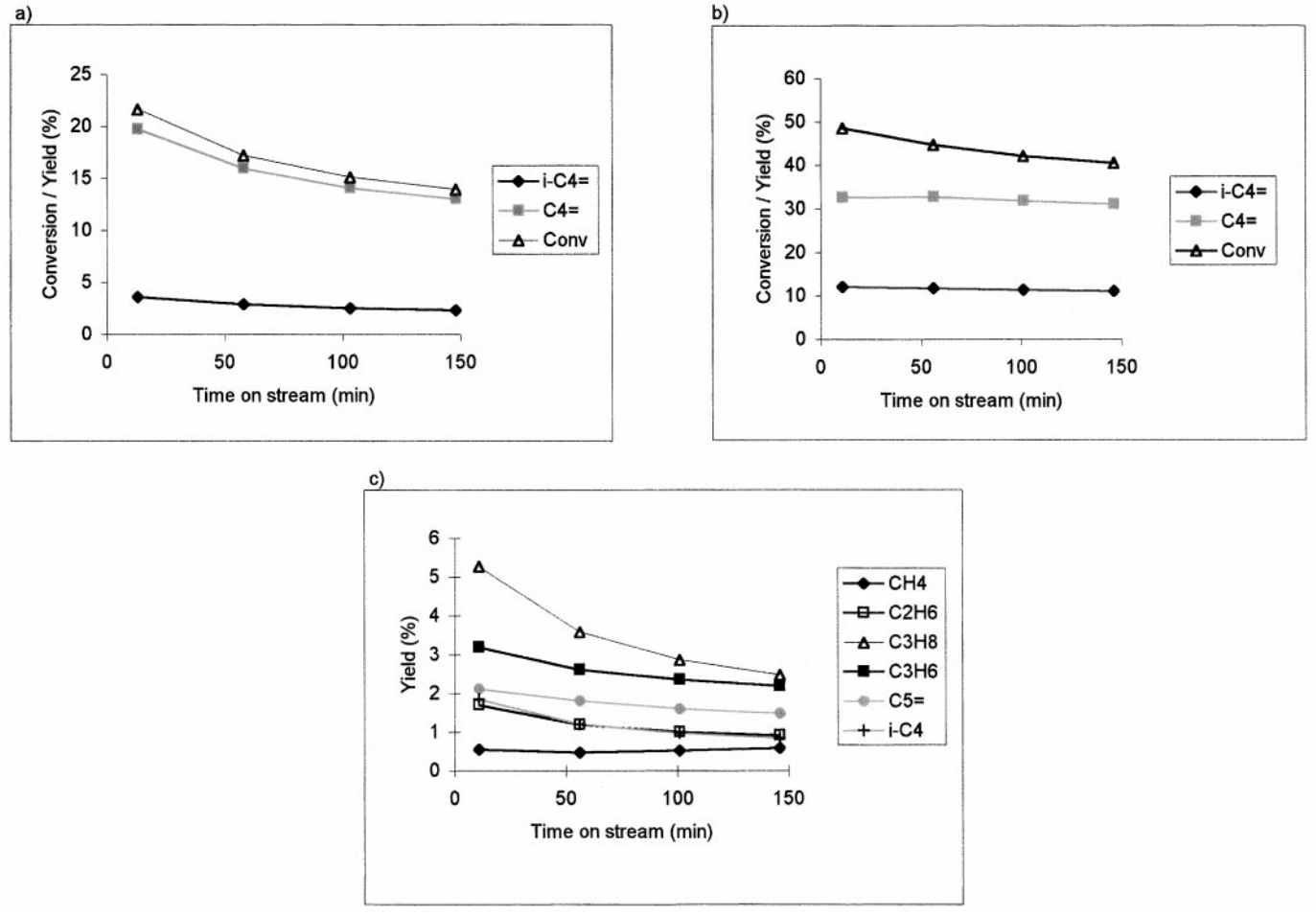

FIG. 1. Conversion and yield of the major products in the dehydroisomerization of *n*-butane over 0.1% Pt–ZSM5(480): 830 K, 1.8 bar, 10% *n*-butane, 20% H_2. (a) WHSV = 86 h^{-1}. (b–c) WHSV = 9.9 h^{-1}.

the ratio $i\text{-}C_4^= / \sum C_4^=$ ("isomer fraction") for two catalysts ZSM5(480) and ZSM5(125), respectively. The conversion, the yield of butenes, and the yield of isobutene increased with metal loading. The small difference in activity between 0.3 and 0.5% Pt–ZSM5(125) was attributed to the rather low dispersion of 0.5% Pt–ZSM5(125). The ratio of isobutene to butene, however, did not vary with metal loading. With increasing space time, it asymptotically approached the thermodynamic equilibrium value of 41%. Note that the material with the higher Brønsted acid site concentration, i.e., ZSM5(125) approached the 41% ratio much faster than ZSM5(480).

Figure 4 compares the yields of total butenes, i.e., the dehydrogenation activity, and the isomer fraction for catalysts with a metal loading of 0.3% Pt, but different acid site concentrations. Figure 5 shows the same comparison for catalysts with a metal loading of 0.5% Pt. Both figures show that (at low space times) the yield of butenes did not depend on the acid site concentration. The isomer fraction, however, increased with the acid site concentration.

The Effect of Conversion on the Selectivity

For all catalysts, the yields of the sum of all butenes and of isobutene passed through a maximum as a function of conversion (see Fig. 6 as an example). At higher conversions, the yields decreased at the expense of an increase in by-product formation. Figure 7 gives an example of the selectivity to *n*-butene, to isobutene, and to the major by-products as a function of conversion. The selectivity to *n*-butene extrapolated to a value between 90 and 100% at zero conversion and the selectivity to isobutene to a value between 0 and 10%. The initial selectivity to by-products was close to zero. With increasing conversion, the selectivity to *n*-butene decreased, while the selectivity to isobutene and to the by-products increased. Finally, also the selectivity to isobutene decreased at the expense of a sharp increase in the selectivity to propane. Propane dominated the by-product spectrum at high conversions, followed by propene, ethane, and isobutane (their order depended on the conversion). The ratios of ethane to ethene, propane to propene,

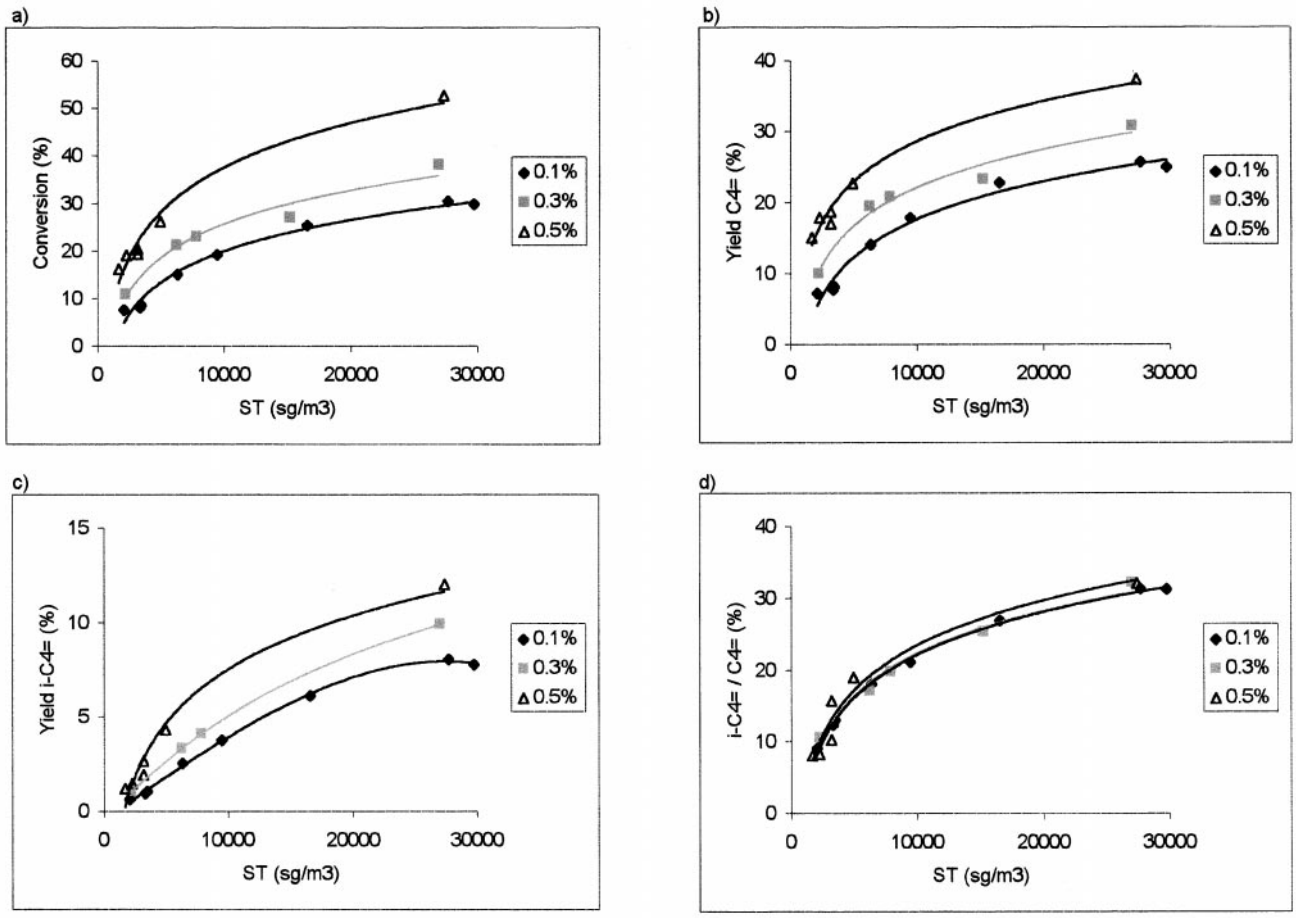

FIG. 2. Catalyst ZSM5(480): (a) conversion, (b) yield of the sum of butenes ($\Sigma C_4^=$), (c) Isobutene yield, and (d) ratio $i\text{-}C_4^=/\Sigma C_4^=$ as a function of space time (ST) and metal loading (830 K, 1.8 bar, 10% *n*-butane, and 20% H_2). $ST = m_{cat}/(dV/dt)$, where m_{cat} is the catalyst mass and (dV/dt) the total flow.

and isobutane to isobutene increased with increasing conversion.

The selectivity was clearly seen to be primarily a function of the ratio between Brønsted acid sites and accessible metal atoms. At a constant acid site concentration, the selectivity to propene decreased and the selectivity to total butenes increased with metal loading. At a constant metal loading, the selectivity to propene increased and the selectivity to total butenes decreased with increasing acid site concentration (see Fig. 8). Other variations were too subtle to be described in detail here.

Butane Conversion over the Parent ZSM5

To evaluate the influence of the zeolite upon the primary conversion of *n*-butane, the catalytic activity and selectivity of the ZSM5 samples were studied. At a WHSV = 10 and 20, under conditions identical to the testing of the bifunctional catalysts, ZSM5(480) gave conversions of only 1.35 and 0.75%, respectively; 0.1% Pt–ZSM5(480) gave conversions of 42 and 31% under the same conditions. The main products of ZSM5(480) were methane, ethane, ethene, and propene resulting from (protolytic) cracking of butane according to Eqs. [2] and [3][2], and butene, formed by acid-catalyzed dehydrogenation, Eq. [4] (18). Table 4 compares the rates of by-product formation in the absence/presence of Pt for two different SiO_2/Al_2O_3 ratios. Generally, the rate was higher for the metal-impregnated samples, even at the lowest metal loading. The difference was largest for propane, ethane, and propene and smallest for ethene and methane.

$$n\text{-}C_4H_{10} \rightarrow CH_4 + C_3H_6 \quad [2]$$

$$n\text{-}C_4H_{10} \rightarrow C_2H_6 + C_2H_4 \quad [3]$$

$$n\text{-}C_4H_{10} \rightarrow C_4H_8 + H_2 \quad [4]$$

[2] The rates of methane and propene and ethane and ethene formation, respectively, did not match completely, as expected from the stoichiometry of the cracking reaction, which means that some secondary reactions were also taking place.

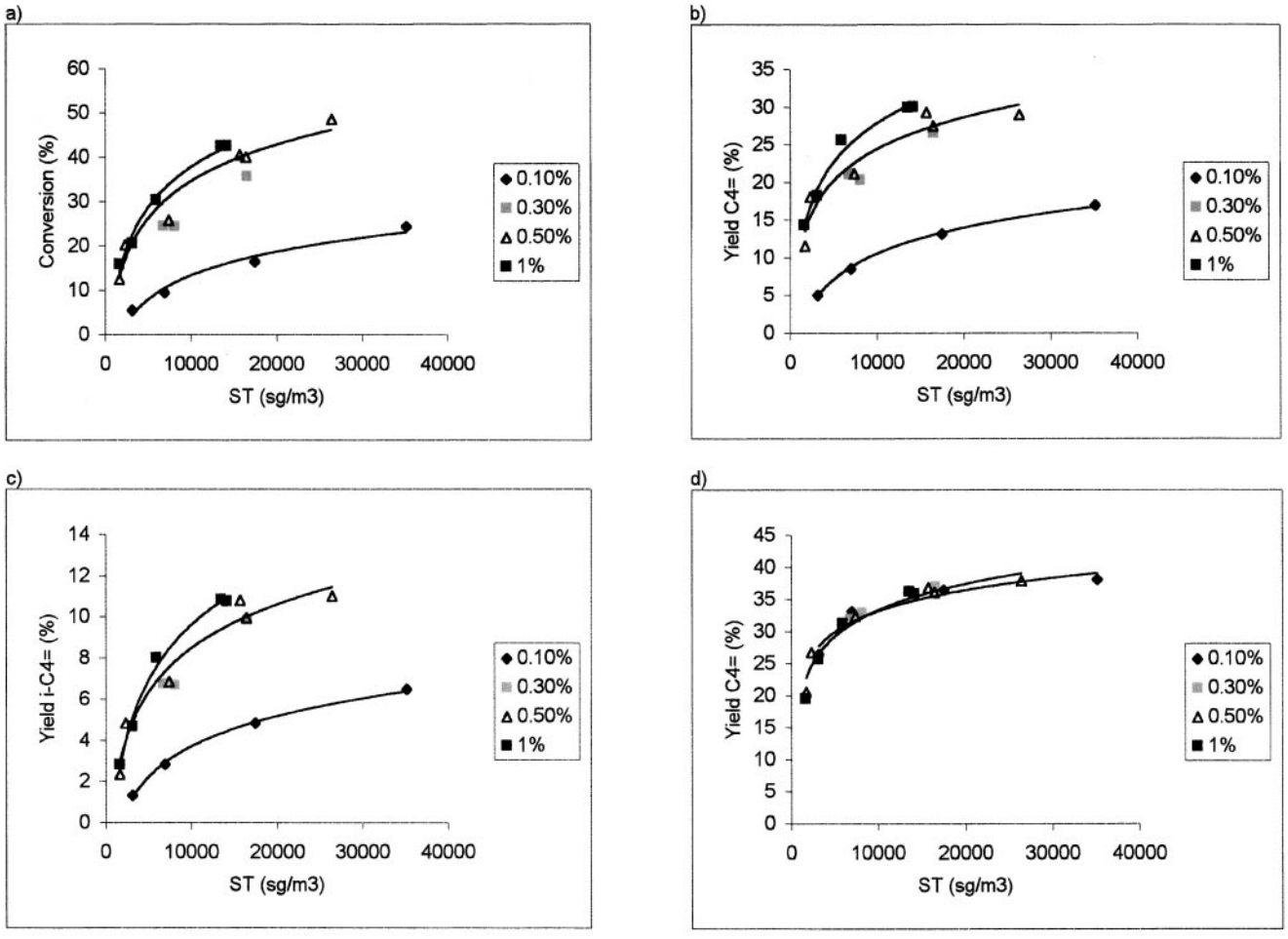

FIG. 3. Catalyst ZSM5(125): (a) conversion, (b) yield of the sum of butenes ($\Sigma C_4^=$), (c) isobutene yield, and (d) ratio $i\text{-}C_4^=/\Sigma C_4^=$ as a function of space time (ST) and metal loading (830 K, 1.8 bar, 10% *n*-butane, and 20% H_2).

DISCUSSION

The Bifunctional Reaction Mechanism

As outlined in the Introduction, the formation of isobutene from *n*-butane over Pt–ZSM5 is expected to proceed via the classical bifunctional mechanism (19). The experimental observations fully support this. At short contact times, the total conversion and the yield of butene increased with metal loading, but were constant for samples which only differed by the amount of acid sites (Figs. 2–5), suggesting that both depend only on the metal loading. In accordance with such a model, a Pt-free ZSM5 showed hardly any conversion of *n*-butane. Thus, dehydrogenation of butane to butene is the primary reaction step and proceeds over Pt.

As the selectivity to isobutene extrapolated to a value close to 0% at zero conversion (Fig. 7), it is concluded to be a secondary product. The ratio of isobutene to the sum of all butenes (isomer fraction) did not depend on the metal loading, but on the concentration of acid sites (Figs. 2–5), indicating that the skeletal isomerization takes place over Brønsted acid sites.

TABLE 4

Rates of By-product Formation and Rate of Dehydrogenation in Conversion of *n*-Butane over (Pt)–ZSM5 (830 K, 1.8 bar, 10% *n*-butane, 20% hydrogen, and 100 min Time on Stream)

Rate of formation (10^{-6} mol/s · g)	ZSM5(480)	0.1% Pt–ZSM5(480)[a]	ZSM5(80)	0.1% Pt–ZSM5(80)[a]
CH_4	0.25	0.9	1.3	2.3
C_2H_6	0.17	0.8	1.2	4.0
C_2H_4	0.19	0.2	1.2	1.3
C_3H_8	0.00	0.4	0.14	4.0
C_3H_6	0.24	1.0	1.2	10
$C_4^=$	0.26	80	1.0	125

[a] Extrapolated to zero conversion.

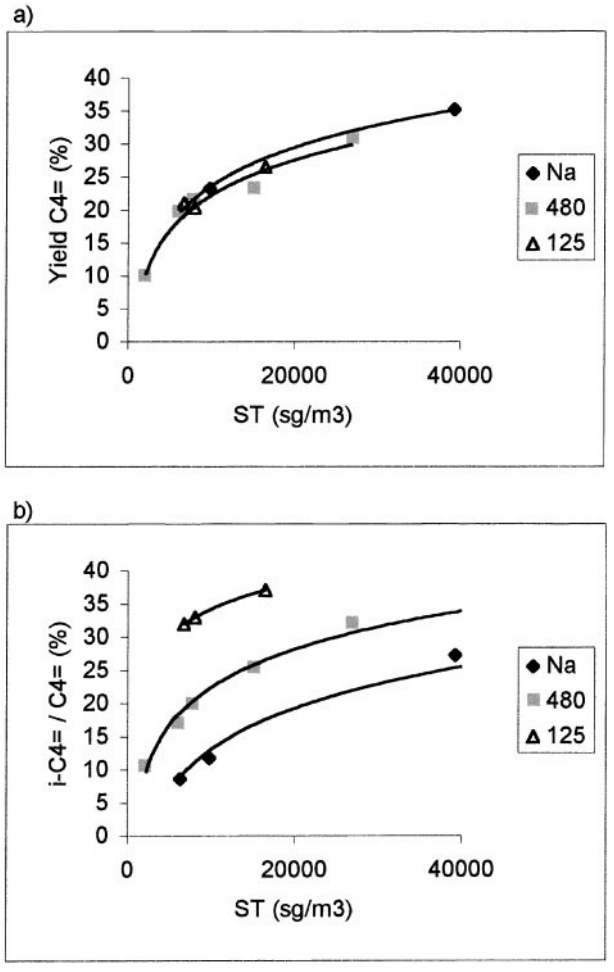

FIG. 4. Symbols: Na = Na-0.3% Pt–ZSM5(480). 480 = 0.3% Pt–ZSM5(480). 125 = 0.3% Pt–ZSM5(125). (a) Yield of the sum of butenes ($\Sigma C_4^=$). (b) Ratio i-$C_4^=/\Sigma C_4^=$. 1.8 bar, 830 K, and 100 min time on stream. Feed: 10% n-butane; 20% H_2.

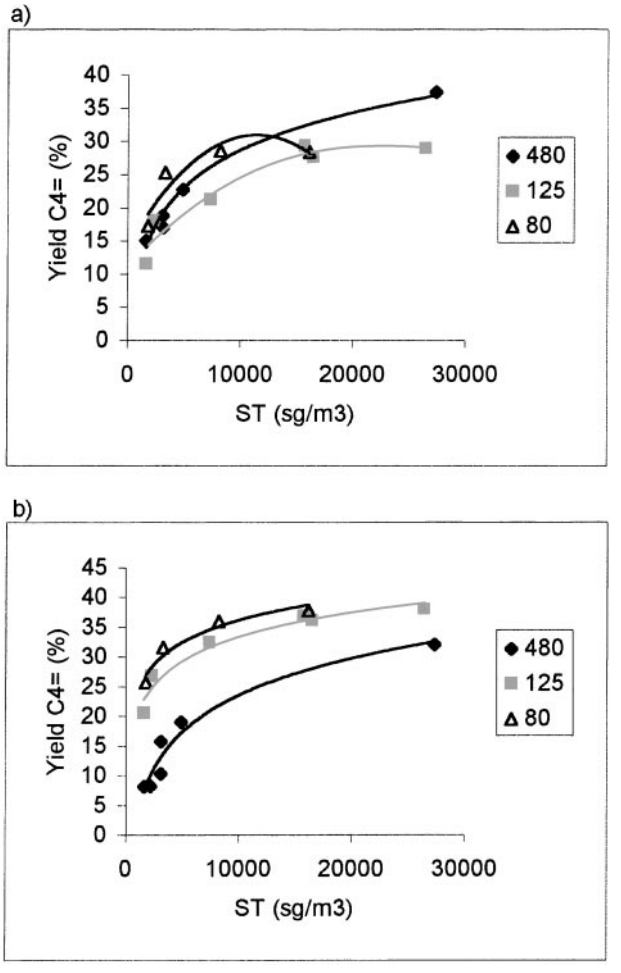

FIG. 5. 0.5% Pt–ZSM5. $SiO_2/Al_2O_3 = 480$ (diamonds); 125 (squares); 80 (triangles). (a) Yield of the sum of butenes ($\Sigma C_4^=$). (b) Ratio i-$C_4^=/\Sigma C_4^=$. 1.8 bar, 830 K, 100 min time on stream. Feed: 10% n-butane; 20% H_2.

The Thermodynamics of Butane Dehydroisomerization

The dehydroisomerization of n-butane involves two equilibrium reactions, i.e., the dehydrogenation of n-butane and the skeletal isomerization of butene.

	$\Delta H_{830\ K}$	$\Delta G_{830\ K}$	K	
n-$C_4H_{10} \Leftrightarrow$ 1-$C_4H_8 + H_2$	131 kJ/mol	17.4 kJ/mol	0.08	[5]
1-$C_4H_8 \Leftrightarrow i$-C_4H_8	−16.1 kJ/mol	−7.4 kJ/mol	2.93	[6]

If residence time of isobutene in the reactor is high enough, it can, of course, be rehydrogenated to isobutane. In that case, also, this equilibrium has to be considered.

	$\Delta H_{830\ K}$	$\Delta G_{830\ K}$	K	
i-$C_4H_8 + H_2 \Leftrightarrow i$-$C_4H_{10}$	−123 kJ/mol	−5.5 kJ/mol	2.21	[7]

Equations [5] and [6] show that dehydroisomerization is

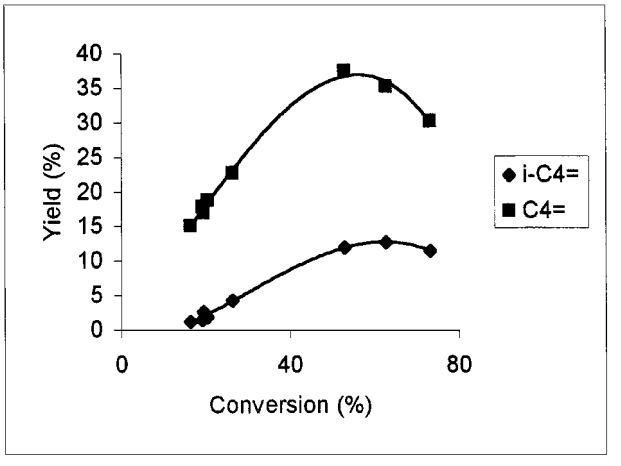

FIG. 6. Catalyst 0.5% Pt–ZSM5(480). Yield of isobutene and the sum of butenes ($\Sigma C_4^=$). 1.8 bar, 830 K, 100 min time on stream. Feed: 10% n-butane; 20% H_2.

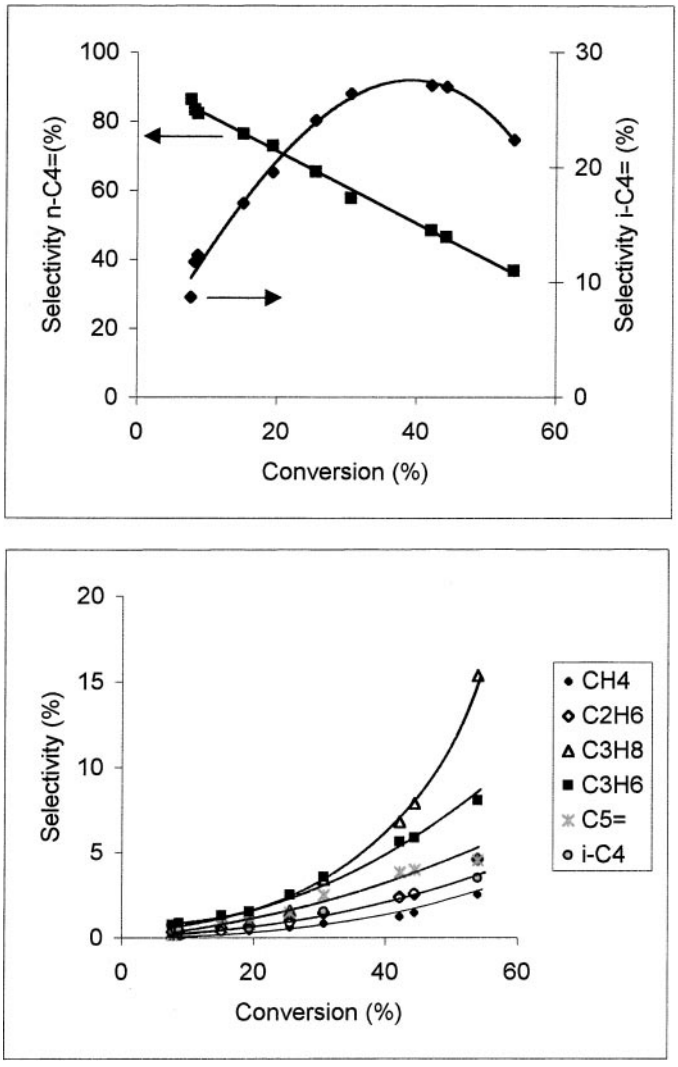

FIG. 7. Catalyst 0.1% Pt–ZSM5(480). Selectivity to the major (by-) products. 1.8 bar; 830 K; 100 min time on stream. Feed: 10% *n*-butane; 20% H_2.

a combination of an endothermic reaction (dehydrogenation), which is favored at high temperatures, and a slightly exothermic reaction (butene isomerization), which is favored at low temperatures. Both equilibria limit the possible yield of isobutene. Figure 9 shows the equilibrium concentration of the sum of linear butenes, isobutene, and butadiene as a function of temperature. If the other parameters (pressure and hydrogen-to-hydrocarbon ratio) are fixed to the values used in the present study, the maximum yield of isobutene is potentially achieved at 900 K. However, at this temperature also large amounts of butadiene will possibly form, which is known to rapidly deactivate acid catalysts. Therefore, 830 K was chosen as a reaction temperature. At 830 K, reasonable yields of isobutene can be achieved (22%), while the yield of butadiene is limited to less than 2% by thermodynamics.

Let us now turn our attention to how the thermodynamic constraints influence the product distribution observed. A direct comparison between thermodynamic calculations and experimental observations has to be done very cautiously, since side reactions are not considered in the calculations. Moreover, the hydrogenation/dehydrogenation equilibria depend on the concentrations of hydrogen and butane/butene, which change in the course of the reaction. A comparison between thermodynamic calculations and experimental results is feasible, however, if only the C_4 fraction of the reactor effluent is considered (i.e., the by-product formation is neglected) and if the hydrogen partial pressure is assumed to be constant at 0.36 bar (the feed value). This is a realistic approximation as the partial pressure of hydrogen additionally produced in the reaction network is marginal compared to the total hydrogen partial pressure. If the hydrogen partial pressure is constant, the equilibrium mole fractions are independent of the hydrocarbon concentration.

For visualization of how the system approaches the thermodynamic equilibrium between *n*-butane, *n*-butene, isobutane, and isobutene, a tetrahedron can be used (see Fig. 10). Every corner of the tetrahedron represents one of the compounds *n*-C_4 (*A*), *n*-$C_4^=$ (*B*), *i*-$C_4^=$(*C*), and *i*-C_4 (*D*). Every mixture of the four compounds is represented by a point in the tetrahedron. The coordinates of a point *X* with the mole fractions x_A, x_B, x_C, and x_D ($\sum x_i = 1$) can be determined from $1-x_D = (\lambda^*\mu)/(\mu^*\mu)$, where λ is the vector from point *X* to the corner *D* and μ is the normal vector from *D* to the opposite plane of the tetrahedron. The three equations for the three independent mole fractions determine the coordinates of point *X*.

The thermodynamic equilibria between *n*-butane and *n*-butene and *n*-butene and isobutene are represented by points *E* and *F* on the corresponding edges of the tetrahedron. Assuming that the system first reaches dehydrogenation equilibrium and only then the formation of isobutene starts, the system will follow the line *AEG*. *G* represents the equilibrium between *n*-butane, *n*-butene, and isobutene.

The reaction data (after 100 min time on stream) are illustrated in the graph using the mole fractions of *n*-butane, *n*-butene, isobutene, and isobutane after normalization to 1 ($\sum x_i = 1$). A series of data points at increasing conversions show how the system approaches equilibrium for four selected catalysts (see Fig. 10). All the data points lie in the corner of the *n*-butane/*n*-butene/isobutene equilibrium, which is further evidence that the reaction proceeds via dehydrogenation and subsequent isomerization. The enlargement of the triangle *AEG* allows one to monitor how the metal loading and acid site concentration affect the pathway of the reaction mixture to thermodynamic equilibrium.

Over 0.5% Pt–ZSM5(480), the reaction mixture first went into the direction of point *E*, the equilibrium point

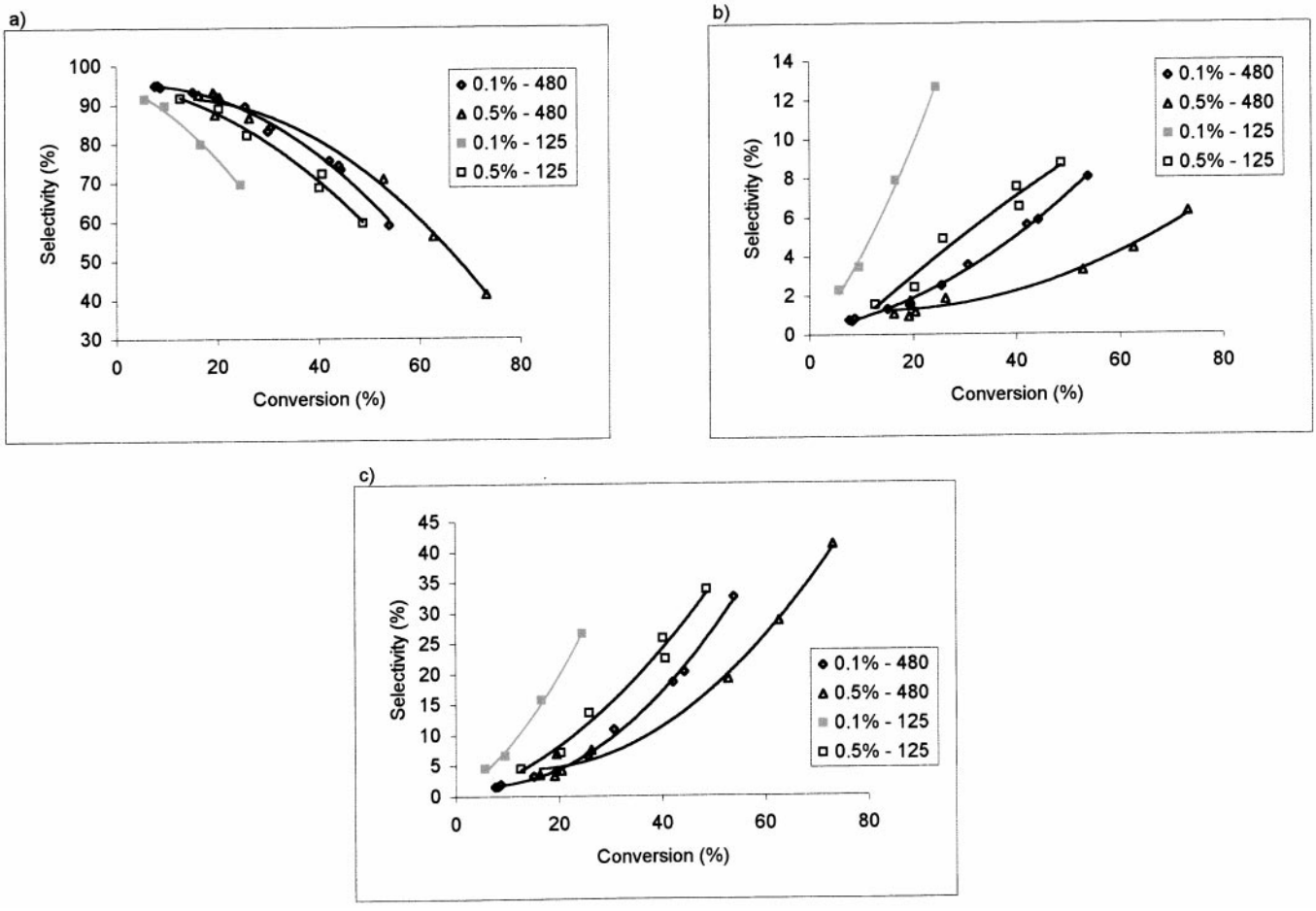

FIG. 8. (a) Selectivity to the sum of butenes ($\Sigma C_4^=$). (b) Selectivity to propene. (c) Summed selectivity to ethane, propane, propene, and pentene. 830 K, 1.8 bar, 100 min time on stream. Feed: 10% *n*-butane; 20% H_2.

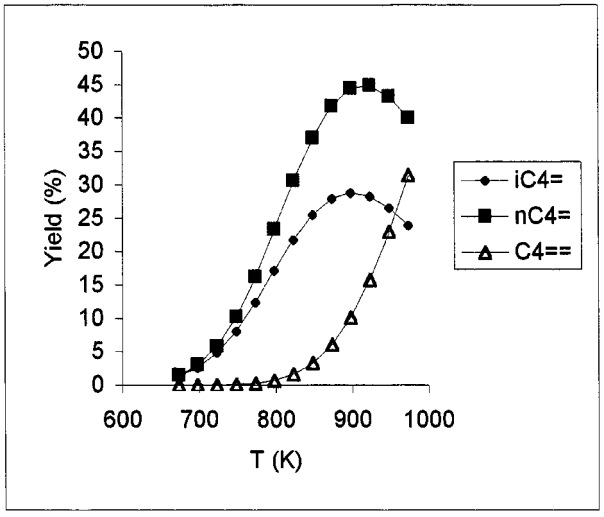

FIG. 9. Dehydrogenation equilibrium as a function of temperature. Pressure set to 1.8 bar. Feed composition: 10% *n*-butane; 20% H_2; 70% N_2. Calculated using HSC Chemistry Version 2.03. Copyright Outokompu Research Oy, Pori, Finland, A. Roine.

between *n*-butane and *n*-butene, before it bent into the direction of *G*. The other extreme behavior was observed with 0.1% Pt–ZSM5(125). The points followed very closely the line *AF* where butene isomerization is in equilibrium. That means that over 0.1% Pt–ZSM5(125) butene isomerization was close to equilibrium from the start of the reaction. The higher the ratio of metal-to-acid sites, the more pronounced was the tendency to reach first the dehydrogenation equilibrium before skeletal isomerization starts. In turn, one can state that the higher the concentration of acid sites, the closer the curves follow first the line of butene isomerization equilibrium. At high conversions, the reaction mixture was quite close to the overall equilibrium point *M*, including isobutane. The highest conversion shown here was 73% for 0.5% Pt–ZSM5(480).

By-product Formation

As side reactions consume a significant fraction of the butenes, it is mandatory to be able to describe and understand these reactions, if the catalyst should be improved.

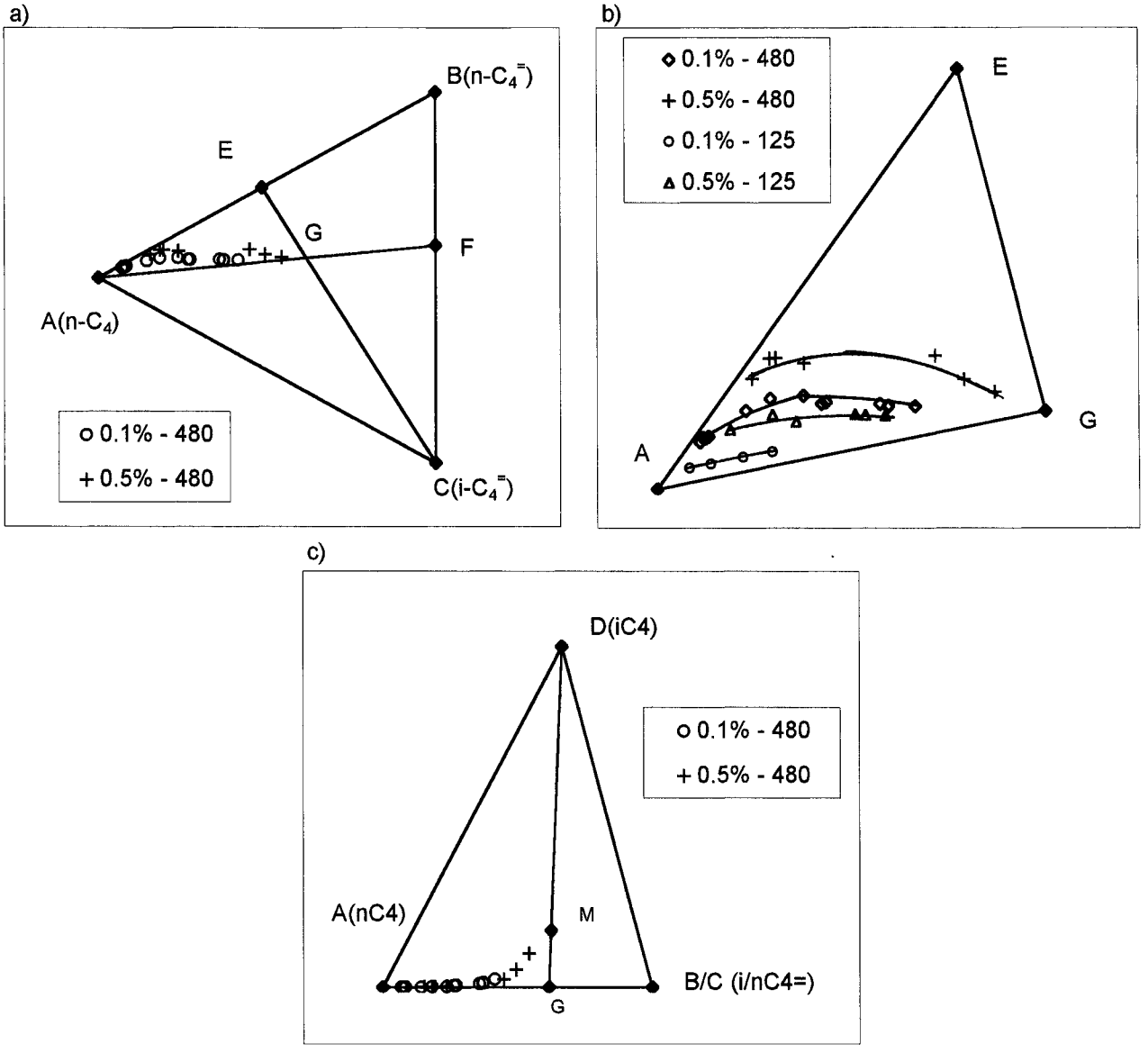

FIG. 10. The *n*-butane/*n*-butene/isobutene/isobutane equilibrium tetrahedron. (a) Projection of the base triangle. (b) Enlargement of the triangle *AEG*. (c) Projection vertical to the base triangle. (*A*) *n*-butane; (*B*) *n*-butene; (*C*) isobutene; (*D*) isobutane; (*E*) equilibrium between *n*-butane and *n*-butene; (*F*) equilibrium between *n*-butene and isobutene; (*G*) equilibrium between *n*-butane, *n*-butene, and isobutene; (*M*) equilibrium between all four compounds.

Conceptually, three routes of by-product formation are conceivable. Their impact will be discussed in the following.

Cracking of Butane over Brønsted Acid Sites

Protolytic cracking of butane over acid sites leads to the formation of methane and propene and ethane and ethene, respectively (20). Ethane and propene were formed much faster in the presence of a metal (see Table 4). Thus, we conclude that these products do not originate from cracking of *n*-butane over the acid sites. The rates of methane and ethene formation, however, were similar in the presence and absence of Pt, indicating that they are at least partly formed by acid-catalyzed cracking. As, even at high conversions, methane and ethene are only minor by-products (see Fig. 7), it is concluded that the contribution of *n*-butane cracking to the overall by-product formation is only minor. It increases, however, with a decreasing SiO_2/Al_2O_3 ratio.

Hydrogenolysis/Isomerization over the Metal

In dehydrogenation reactions over nonacidic, supported metal catalysts, hydrogenolysis and isomerization are the

TABLE 5

Ratio of Metal-to-Acid Sites

Sample	Accessible Pt/H^+
0.5% Pt–ZSM5(480)	0.34
0.1% Pt–ZSM5(480)	0.066
0.5% Pt–ZSM5(125)	0.063
0.1% Pt–ZSM5(125)	0.018

main side reactions (21) of dehydrogenation. Hydrogenolysis leads to the formation of methane, ethane, and propane, metal-catalyzed isomerization and to the formation of isobutane (22–25). Also, here, hydrogenolysis is a primary reaction pathway which competes with dehydrogenation over the metal. However, the selectivities to possible hydrogenolysis products and to isobutane were very low at zero conversion, less than 1% for 0.1% Pt–ZSM5(480) while the selectivity to butenes was around 95%; 0.5% Pt–ZSM5(480) had a higher initial selectivity to methane, ethane, and propane, but still less than 2% each. This indicates that also hydrogenolysis of butane (like butane cracking) does not significantly contribute to the by-product formation. The higher rate of methane formation in the presence of Pt (see Table 5), however, indicates that some hydrogenolysis takes place. Its contribution to the by-product spectrum may increase at high conversions since the competing dehydrogenation reaction is gradually slowed down as it approaches equilibrium (18).

Secondary Reactions of Butenes

The very low initial selectivity to by-products and the sharp increase at high conversions (Fig. 7) indicate that most by-products originate from secondary reactions, i.e., reactions of the butenes formed by dehydrogenation over Pt. Butenes are significantly more reactive than butane. The reaction of butene on acidic zeolites has been extensively studied (26–35) and reviewed (36, 37). The main side reaction competing with skeletal isomerization is di- and oligomerization of the butenes followed by cracking. The main products resulting are propene and pentene, to a smaller extent also ethene and hexene and higher hydrocarbons (see for example, Ref. (37)).

Indeed, propene and pentenes were always found to be by-products of dehydroisomerization here. The molar ratio of $C_3^=/C_5^=$ was much higher than 1, indicating that most of the propene is formed by cracking of larger oligomers than that of C_8 dimers (20, 35) and/or that pentene cracks further to propene and ethene. The selectivity to propene increased with conversion, as expected for a secondary product. However, at high conversions, more propane was formed than propene (see Fig. 7). This is tentatively explained by the fact that propene is hydrogenated to propane in the presence of Pt. The thermodynamic equilibrium ratio of propane to propene at reaction conditions was calculated to be around 70. The experimentally observed ratio was well below that. It increased with increasing conversion. Thus, we conclude that propane is mainly formed by the hydrogenation of propene over Pt.

Similarly, we suggest that isobutane is formed by the hydrogenation of isobutene (38) and not by direct isomerization of *n*-butane over the acid and/or the metal sites and that ethane is formed by the hydrogenation of ethene rather than by hydrogenolysis of butane. However, low concentrations of pentanes and hexanes were found in the products. This is due to thermodynamics. The lower the carbon number, the more favorable it is to hydrogenate the alkene, in line with the decreasing alkane/alkene ratio in the order $C_2 > C_3 > C_4 > C_5$.

The formation of ethane, propane, and isobutane by the hydrogenation of the corresponding alkenes was confirmed by the similarity of the by-product pattern when 1-butene was converted over Pt–ZSM5 in the presence of hydrogen (39).

Influence of Metal Loading and Acid Site Concentration on the Selectivity Pattern

Up to now, dimerization/cracking of butenes over the acid sites has been identified as the major route of by-product formation. Moreover, propane and ethane were identified as products of the dimerization/cracking route. Thus, the selectivities to these four products were lumped into a selectivity to secondary cracking, shown in Fig. 8c. The figure shows that the trend in the selectivity pattern follows closely the trend in the ratio between accessible Pt surface atoms and acid sites (see Table 5). The selectivity to secondary cracking decreases parallel to a increasing ratio of metal-to-acid sites, the selectivity to dehydrogenation increases.

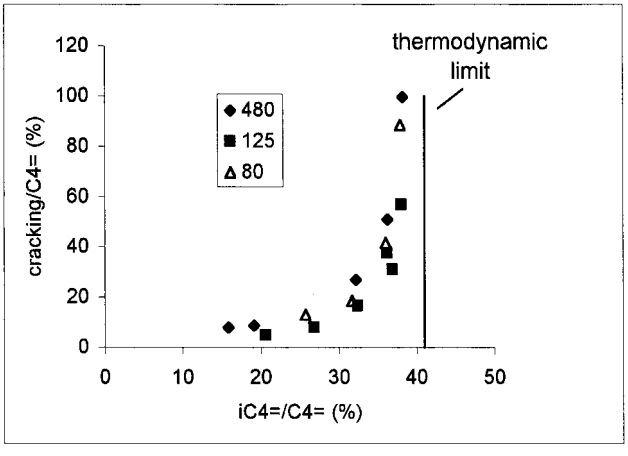

FIG. 11. 0.5% Pt–ZSM5. $SiO_2/Al_2O_3 = 480$ (diamonds); 125 (squares); 80 (triangles). Ratio of the products of secondary cracking to $\Sigma C_4^=$ vs the ratio $i\text{-}C_4^=/\Sigma C_4^=$. 1.8 bar; 830 K; 100 min time on stream. Feed: 10% *n*-butane; 20% H_2.

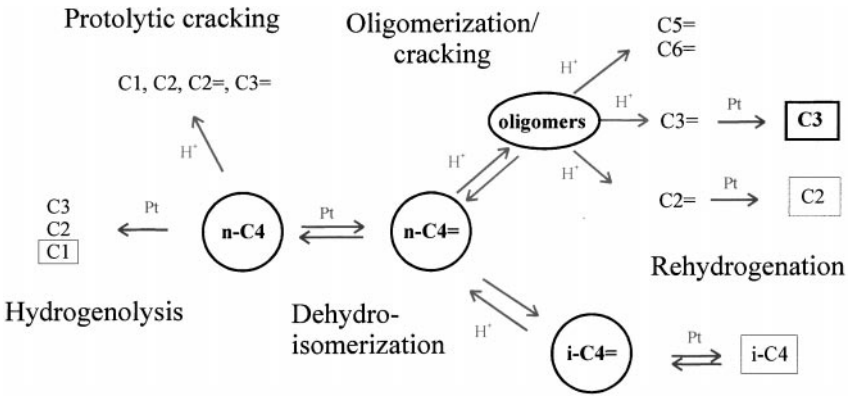

SCHEME 1

Catalysts with a high Brønsted acid site concentration approach the isomerization equilibrium quite fast. The marked increase in the selectivity to dimerization/cracking under such conditions is explained by the fact that the net rate of further isomerization approaches zero, while the side reactions proceed at an unlimited rate. Consequently, the lower the ratio of metal-to-acid sites, the lower is the yield of dehydrogenated products at the point when the selectivity to secondary cracking increases drastically. Thus, it is concluded that a high ratio of metal-to-acid sites is beneficial for catalyst performance. Note that the highest yield of isobutene had been achieved with 0.5% Pt–ZSM5(480), the catalyst with the highest ratio of metal-to-acid sites.

It should, however, be emphasized that the correlation between the Pt/H^+ ratio and the selectivity is only qualitative. For example, 0.5% Pt–ZSM5(125) had almost the same ratio of Pt/H^+ as 0.1% Pt–ZSM5(480), but still a lower selectivity to dehydrogenation. This is due to the contribution of other side reactions, i.e., hydrogenolysis and protolytic cracking of *n*-butane. 0.5% Pt–ZSM5(125) has a higher metal loading and a higher acid site concentration than 0.1% Pt–ZSM5(480), leading to a higher contribution of these two reactions and, thus, a lower selectivity. In addition to these observations, we would like to note that the initial values (at zero time on stream) of the selectivity to by-products were higher, but otherwise the same trends were observed as those for the steady state values.

CONCLUSIONS

The dehydroisomerization of butane proceeds via a bifunctional mechanism. *n*-butane is dehydrogenated over the metal and is then isomerized over the Brønsted acid sites of the zeolite. The catalytic activity is governed by the metal loading. The concentration of acid sites, on the other hand, determines how much of the primarily formed *n*-butene is converted to isobutene.

The main route of by-product formation is oligomerization/cracking of the primarily formed butenes. Cracking of the oligomers mainly leads to propene which in the presence of Pt is hydrogenated to propane (main by-product at high conversion (see Scheme 1)). The overall selectivity of the catalyst is governed by the ratio of metal-to-acid sites. The higher the ratio, the higher the selectivity to dehydrogenation and the lower the selectivity to secondary cracking. Thus, a high ratio of metal-to-acid sites is important for successful catalysts.

ACKNOWLEDGMENTS

This work was performed under the auspices of NIOK, the Netherlands Institute of Catalysis Research. IOP Katalyse (IKA 94023) is gratefully acknowledged for financial support.

REFERENCES

1. Obenaus, F., Droste, W., and Neumeister, J., *in* "Ullmann's Encyclopedia of Industrial Chemistry" (W. Gerhartz, Y. St. Yamamoto, F. T. Campbell, R. Pfefferkorn, and J. F. Rounsaville, Eds.), 5th ed., Vol. A4, p. 491. VCH, Weinheim, 1985–1986.
2. Energy Security Analysis, Inc., "Supply and cost of alternatives to MTBE in gasoline, Report on the Oxygenate Market: Current Production Capacity, Future Supply Prospects and Costs Estimates." Energy Security Analysis, Inc., Wakefield, MA, October 1998 (prepared for the California Energy Commission).
3. Sissel, K., *Chem. Week* **161**(13), 7 (1999).
4. Bellussi, G., Giusti, A., and Zanibelli, L., U.S. Patent 5.336.830 (1994) (assigned to Eniricerche S.p.A. and Snamprogetti S.p.A.).
5. Nagata, H., Iguchi, T., Takiyama, Y., Kishida, M., and Wakabayashi, K., *in* "Book of Abstracts, 11th International Zeolite Conference, Seoul, Korea, 1995," p. RP120.
6. Byggningsbacka, R., Kumar, N., and Lindfors, L.-E., *Catal. Lett.* **55**, 173 (1998).
7. de Agudelo, M. M., Romero, T., Guaregua, J., and Gonzalez, M., U.S. Patent 5.416.052 (1995) (assigned to Intevep, S.A.).
8. Kolombos, A. J., Telford, C. D., and Young, D., European Patent 42.252 (1981) (assigned to The British Petroleum Company Limited).
9. Shum, V. K., U.S. Patent 4.962.266 (1990) (assigned to Amoco Corp.).
10. O'Young, Ch.-L., Browne, J. E., Matteo, J. F., Sawicki, R. A., and Hazen, J., U.S. Patent 5.198.597 (1993) (assigned to Texaco Inc.).
11. Houzvicka, J., Klik, R., Kubelkova, L., and Ponec, V., *Appl. Catal. A* **150**, 101 (1997).

12. Kaminsky, M. P., Froment, G. F. A., and deHertog, W. J. H., WO 93/15835 (1993) (assigned to Amoco Corp.).
13. Che, M., and Bennett, C. O., *Adv. Catal.* **36**, 55 (1989).
14. Le Page, J.-F., Cosyns, J., Courty, P., Freund, E., Franck, J.-P., Jacquin, Y., Juguin, B., Marcilly, C., Martino, G., Miquel, J., Montarnal, R., Sugier, A., and van Landeghem, H., *in* "Applied Heterogeneous Catalysis," p. 113. Editions Technip, Paris, 1978.
15. van den Broek, A. C. M., van Grondelle, J., and van Santen, R. A., *J. Catal.* **167**, 417 (1997).
16. Englisch, M., Ph.D. thesis, University of Twente, Enschede, The Netherlands, 1996.
17. Eder, F., Ph.D. thesis, University of Twente, Enschede, The Netherlands, 1996.
18. Narbeshuber, T. G., Vinek, H., and Lercher, J. A., *J. Catal.* **157**, 388 (1995).
19. Weisz, P. B., *Adv. Catal.* **13**, 137 (1962).
20. Haag, W. O., and Dessau, R. M., *in* "Proceedings, 8th International Congress on Catalysis, Berlin, 1984," Vol. II, p. 305. Dechema, Frankfurt am Main, Berlin, 1984.
21. Corthright, R. D., and Dumesic, J. A., *J. Catal.* **148**, 771 (1994).
22. Bond, G. C., and Gelsthorpe, M. R., *J. Chem. Soc., Faraday Trans. 2* **85**, 3767 (1989).
23. Bond, G. C., and Yide, Xu, *J. Chem. Soc., Faraday Trans. 1* **80**, 969 (1984).
24. Kempling, J. Ch., and Anderson, R. B., *Ind. Eng. Chem. Process Res. Dev.* **11**, 146 (1972).
25. Sinfelt, J. H., *Adv. Catal.* **23**, 91 (1973).
26. Guisnet, M., Andy, P., Gnep, N. S., Benazzi, E., and Travers, C., *J. Catal.* **158**, 551 (1996).
27. Mériaudeau, P., Tuan, V. A., Le, N. H., and Szabo, G., *J. Catal.* **169**, 397 (1997).
28. Houzvicka, J., Hansildaar, S., and Ponec, V., *J. Catal.* **167**, 273 (1997).
29. Xu, W.-Q., Yin, Y.-G., Suib, L., Edwards, J. C., and O'Young, Ch.-L., *J. Phys. Chem.* **99**, 9443 (1995).
30. O'Young, Ch.-L., Pellet, R. J., Casey, D. G., Ugolini, J. R., and Sawicki, R. A., *J. Catal.* **151**, 467 (1995).
31. Xu, W.-Q., Yin, Y.-G., Suib, St. L., and O'Young, Ch.-L., *J. Catal.* **150**, 34 (1994).
32. Simon, M. W., Suib, St. L., and O'Young, Ch.-L., *J. Catal.* **147**, 484 (1994).
33. Byggningsbacka, R., Lindfors, L. E., and Kumar, N., *Ind. Eng. Chem. Res.* **36**, 2990 (1997).
34. Mooiweer, H. H., de Jong, K. P., Kraushaar-Czarnetzki, B., Stork, W. H. J., and Krutzen, B. C. H., *Stud. Surf. Sci. Catal.* **84**, 2327 (1994).
35. Asensi, M. A., Corma, A., and Martinez, A., *J. Catal.* **158**, 561 (1996).
36. Butler, A. C., and Nicolaides, C. P., *Catal. Today* **18**, 443 (1993).
37. Houzvicka, J., and Ponec, V., *Catal. Rev.-Sci. Eng.* **39**, 319 (1997).
38. Sad, M. R., Querini, C. A., Comelli, R. A., Figoli, N. S., and Parera, J. M., *Appl. Catal. A* **146**, 131 (1996).
39. Pirngruber, G. D., Seshan, K., and Lercher, J. A., "The Conversion of Butene over Pt-ZSM5," unpublished results.